

**Facile Template-Assisted Synthesis of PtBiTe Nanoplates for CO-Free Methanol Oxidation in
Alkaline Electrolytes**

Xinyu Huo, Baomin Luo*, Yezhen Zhang, Hanshuo Li

College of Chemistry and Pharmacy Engineering, Nanyang Normal University, 473061 Nanyang, PR
China

*Corresponding author: bmluo@nynu.edu.cn (B. Luo)

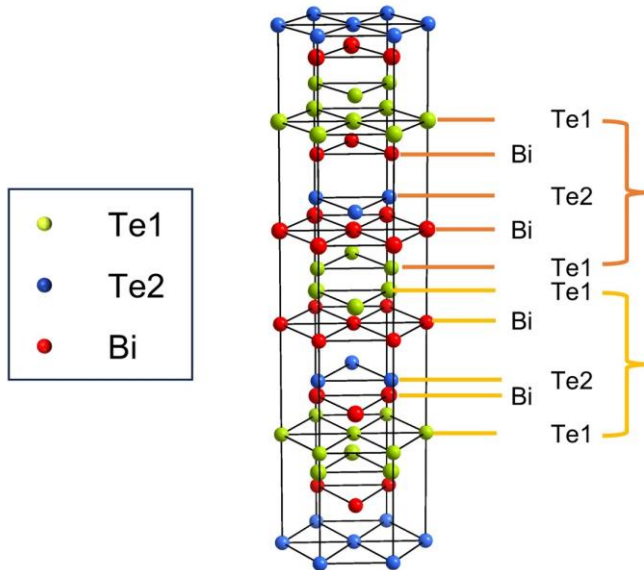


Fig. S1 The unit cell of the hexagonal Bi_2Te_3 .

There are 18 Bi atoms and 27 Te atoms in the hexagonal Bi_2Te_3 unit cell, and the atomic ratio of Bi to Te is 2:3. The atomic arrangement in the hexagonal Bi_2Te_3 can be visualized in terms of the layer structure. Essentially, this consists of a stacking of “quintuple layer” leaves. In each leaf, the layers occur in the order –Te1–Bi–Te2–Bi–Te1–. Here, 1 and 2 are used to distinguish two types of differently bonded Te atoms. Each Te2 atom is surrounded by six Bi atoms, whereas the Te1 atoms have three nearest-neighbour Bi atoms at the same leaf and three next nearest Te atoms in the adjacent leaf.^[1-5]

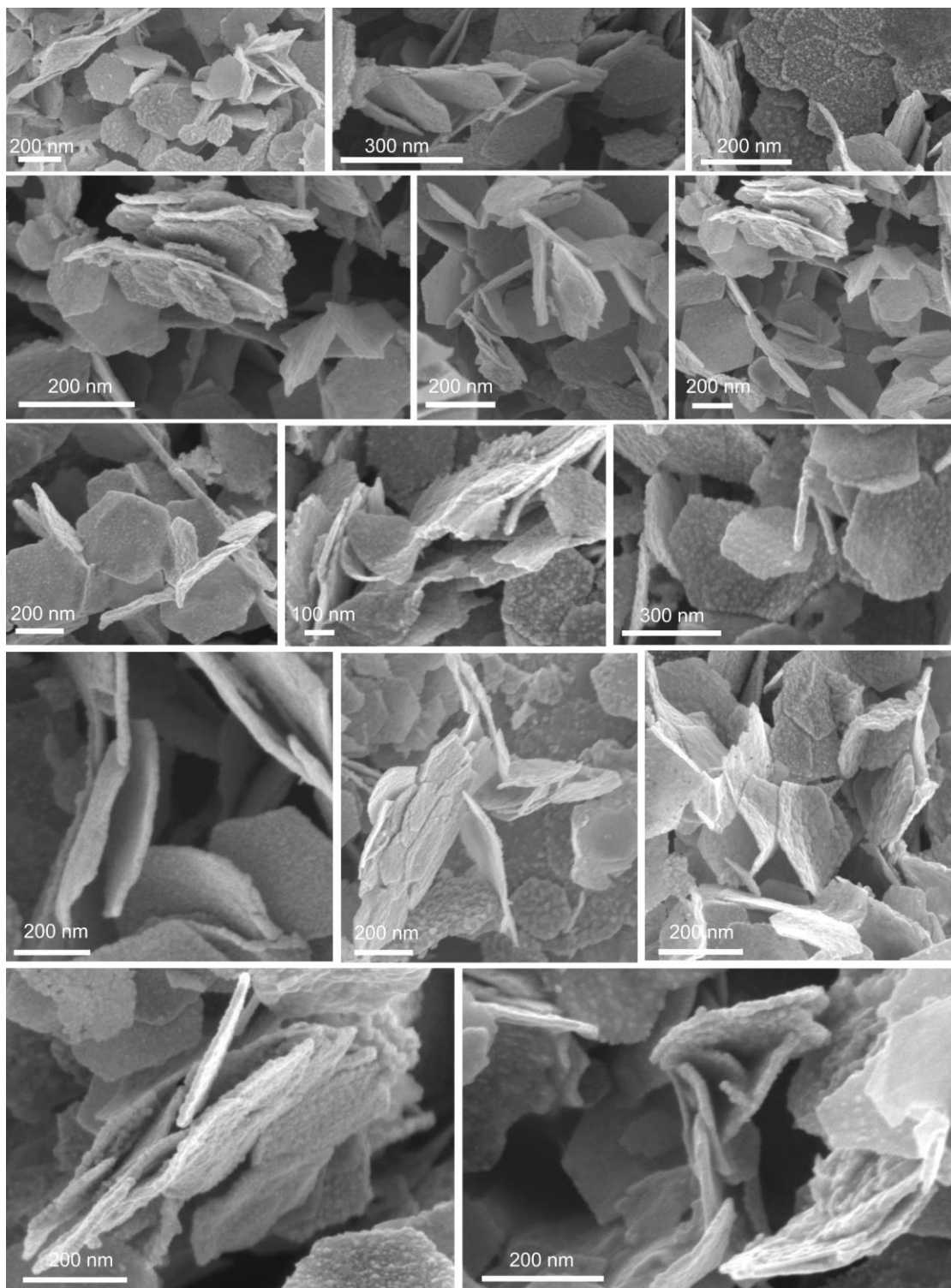


Fig. S2 FESEM images of the PtBiTe NPs for the thickness statistic (Part one).

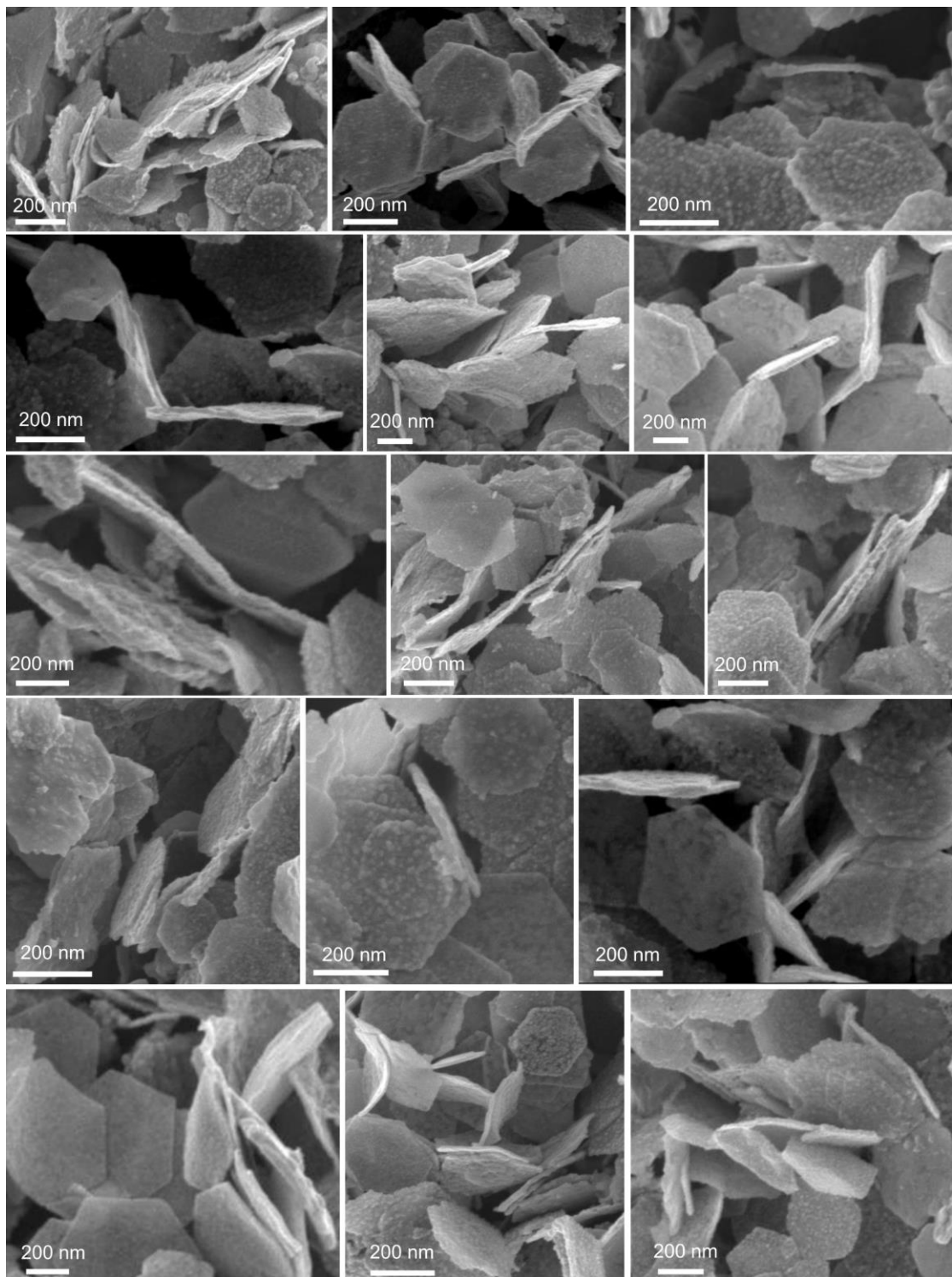


Fig. S3 FESEM images of the PtBiTe NPs for the thickness statistic (Part two).

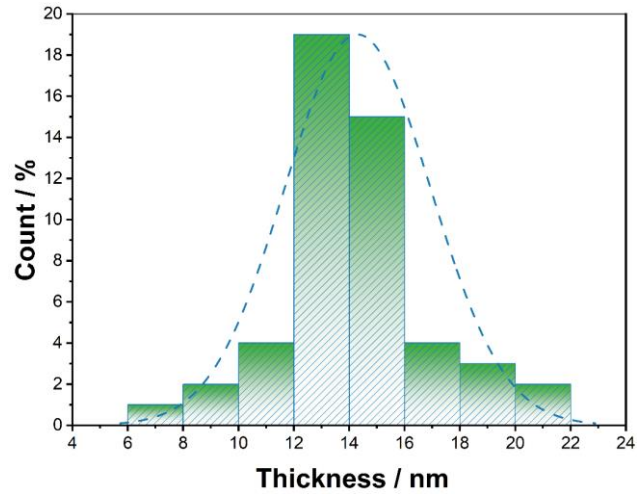


Fig. S4 Histogram of the thickness distribution of the PtBiTe NPs.

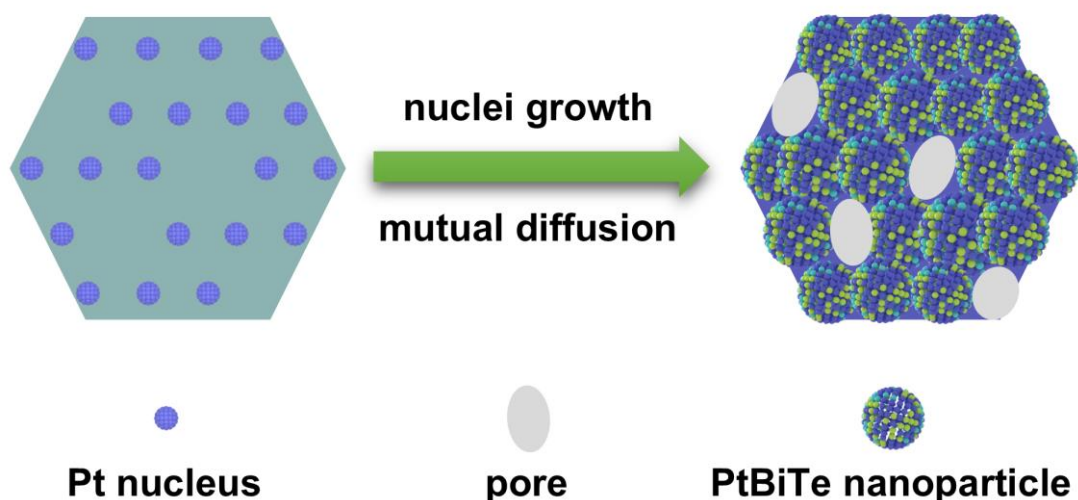


Fig. S5 Schematic diagram of the formation mechanism of the PtBiTe NPs.

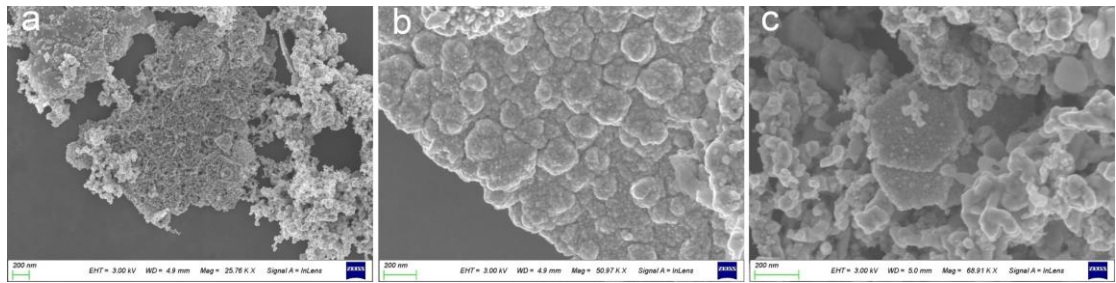


Fig. S6 FESEM images of the PtBiTe catalysts synthesized in different solvents, (a) DMF, (b) ethanol, and (c) glycerol.

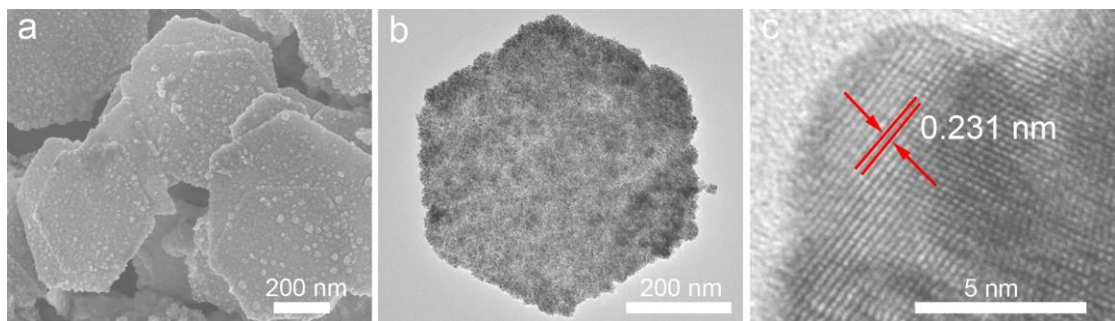


Fig. S7 (a) FESEM image, (b) TEM image, and (c) HRTEM image of the PtTe NPs.

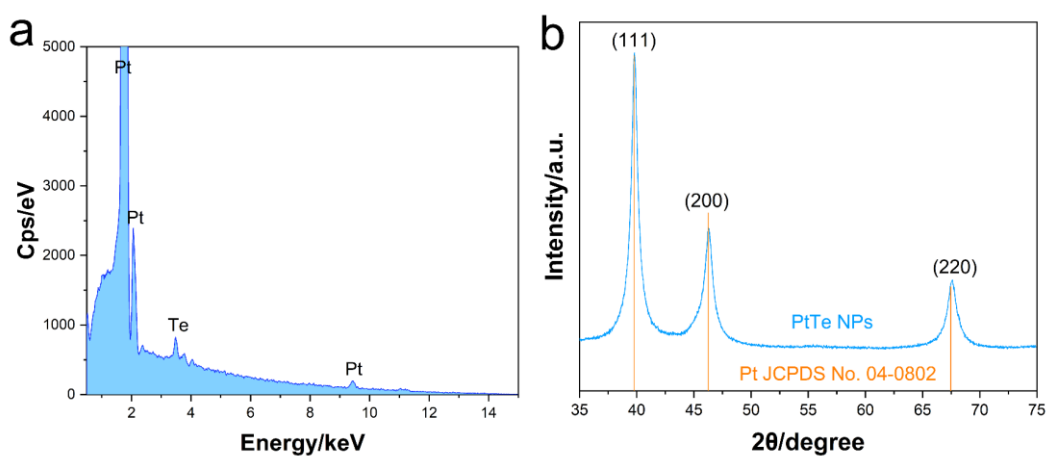


Fig. S8 (a) EDS spectrum and (b) XRD pattern of the PtTe NPs.

Table S1. Theoretical and actual components of the PtBiTe NPs

	Pt (wt%)	Bi (wt%)	Te (wt%)
theoretical components	62.20	19.73	18.07
actual components	67.75	18.03	14.22

Table S2. Summary of peak positions

	PtBiTe NPs	PtTe NPs	Pt/C
Pt (eV)	71.27/74.57	71.38/74.77	71.00 /74.4
PtO (eV)	72.69/75.69	73.10/76.60	72.38/75.77
Bi (eV)	157.28/162.58	—	—
Bi₂O₃ (eV)	158.83/164.13	—	—
Te (eV)	572.96/583.42	573.93/584.41	—
TeO₂ (eV)	575.58/585.97	575.93/586.33	—

Table S3. Atomic percentage of zero-valent atoms and oxidized atoms

	PtBiTe NPs	PtTe NPs	Pt/C
Pt (%)	70.91	80.99	66.16
PtO (%)	29.09	19.01	33.85
Bi (%)	16.23	—	—
Bi₂O₃ (%)	83.77	—	—
Te (%)	46.13	20.21	—
TeO₂ (%)	53.87	79.79	—

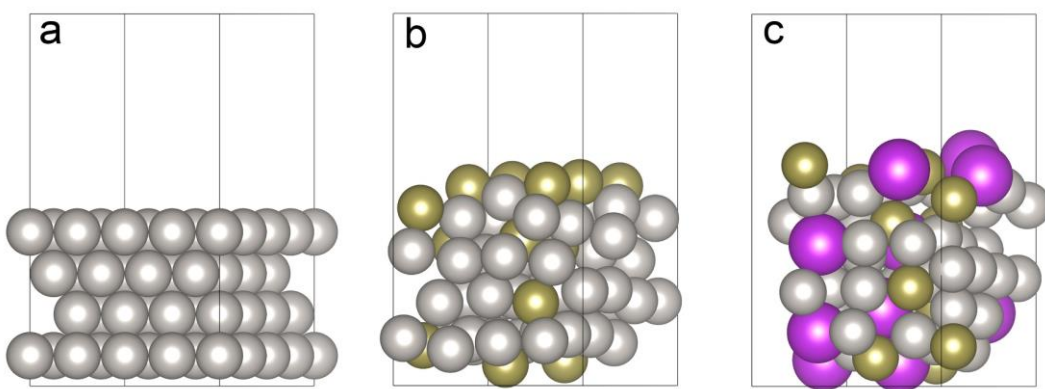


Fig. S9 Structural model of (a) the Pt/C, (b) the PtTe NPs, and (c) the PtBiTe NPs for the PDOS and the Pt d-band center calculation.

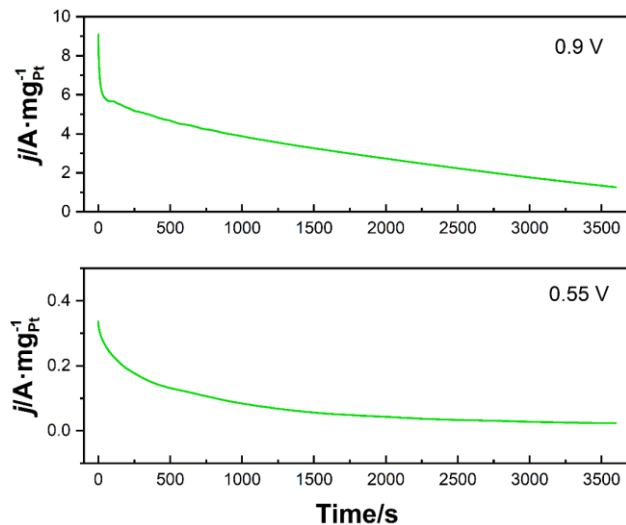


Fig. S10 CA curves of the PtBiTe NPs tested at 0.9 V and 0.55 V.

Table S4. Current retention rates of the PtBiTe NPs under different test potentials

Potential	0.1 s	10 s	Retention rate
0.55 V	0.33665	0.30380	90.2%
0.9 V	9.09000	6.90500	76.0%

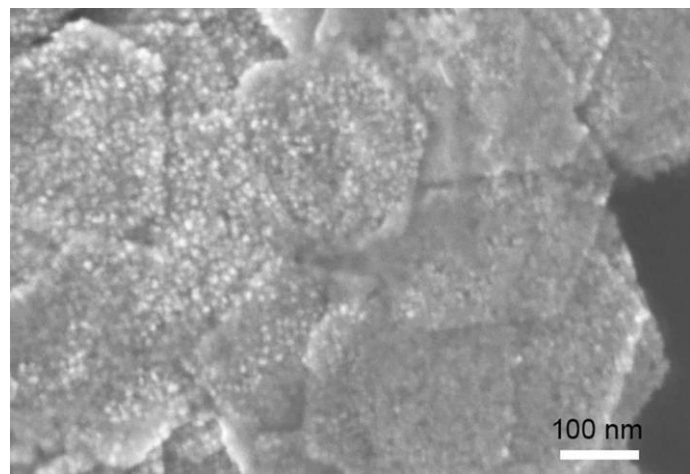


Fig. S11 FESEM of the PtBiTe NPs after the series of electrochemical tests.

Table S5. A comparison of catalytic performance of typical Pt-based catalysts for methanol oxidation

Catalysts	Mass activity (A·mg ⁻¹ _{Pt})	Specific activity (mA·cm ⁻² _{Pt})	E (V vs. RHE)	References
PtBiTe NPs	8.23	37.24	No	This work
PtTe NPs	4.35	17.86	0.42	This work
Pt ₃ Ni nanowires	1.737	5.926	—	[6]
Pt ₁₆ Te Nanotroughs and Nanopillars	3.20	9.8	—	[7]
PtAuNi hollow nanospheres	1.184	31.52	0.421	[8]
Pt-NiO nanochains	0.88	—	—	[9]
Pt nanoparticles/Te rods	0.82	1.13	—	[10]
PtCu nanodendrites	0.88	2.49	—	[11]
Pt/Ni MOF/rGO	3.49	5.39	0.514	[12]
Pt-CoOOH-CDs/C	0.86	—	0.477	[13]
PtBi/graphene	2.00	—	0.597	[14]
ZIF@PDA/Pt-5-900	1.71	2.6	—	[15]
Pt _{0.13} /Ni-NC	1.9	—	0.40	[16]
PtBi nanorings	6.42	11.93	No	[17]
PtCuNi Tetrahedra	7	14	—	[18]
Pt ₂ Bi nanoparticles	4.6	—	No	[19]
PtPdNi hollow nanospheres	3.95	10.68	0.42	[20]
Pd@Pt core-shell nanoparticles	3.68	24.35	—	[21]
PtAg nanowires	2.22	13	0.68	[22]
Cu-incorporated PtBi nanofibers	6.79	11.28	No	[23]
PtBi nanoparticles	4.5	—	No	[24]
PtBiCu nanoparticles	5.41	20.3	No	[25]

The performances of the listed catalysts were all tested under the same testing conditions, namely in a 1.0 M KOH + 1.0 M CH₃OH electrolyte, with a CV scanning rate of 50 mV·s⁻¹ and at room temperature. In Table S5, E is the onset potential of CO oxidation. No means there is no CO-poisoning issue for this catalyst.

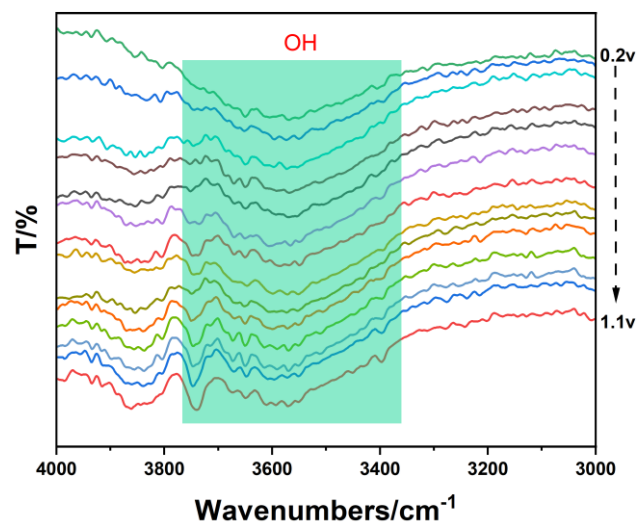


Fig. S12 In situ FTIR spectra (3000~4000 cm⁻¹) of the PtBiTe NPs in 1.0 M KOH + 1 M CH₃OH.

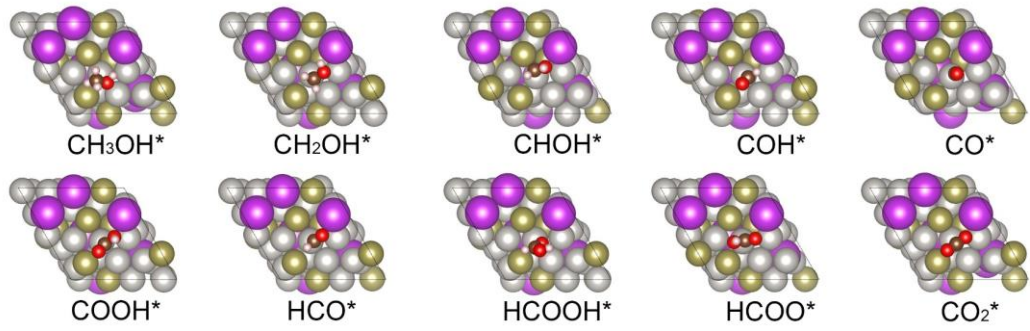


Fig. S13 Optimized structures of intermediates on the PtBiTe slab for the Gibbs free energy calculation.

References

- [1] J. R. Drabble, and C. H. L. Goodman, *J. Phys. Chem. Solids*, 1958, **5**, 142–144.
- [2] Y. Hosokawa¹, K. Tomita, M. Takashiri, *Sci. Rep.-UK*, 2019, **9**, 10790.
- [3] T. Fang, X. Li, C. Hu, Q. Zhang, J. Yang, W. Zhang, X. Zhao, D. J. Singh and T. Zhu, *Adv. Funct. Mater.*, 2019, 1900677.
- [4] Z. Ju, C. Crawford, J. Adamczyk, E. S. Toberer and S. M. Kauzlarich, *ACS Appl. Mater. Interfaces*, 2022, **14**, 24886–24896.
- [5] J. Kampmeier, S. Borisova, L. Plucinski, M. Luysberg, G. Mussler and D. Grützmacher, *Cryst. Growth Des.*, 2015, **15**, 390–394.
- [6] Z. Li, K. Yu, Y. Leng and Z. Chen, *J. Electroanal. Chem.*, 2025, **980**, 118989.
- [7] W. Geng, Y. Zhang, L. Yu, Dr. Li, J. Sang and Y. Li, *Small*, 2021, 2101499.
- [8] C. Liu, Z. Chen, D. Rao, J. Zhang, Y. Liu, Y. Chen, Y. Deng and W. Hu, *Sci. China Mater.* 2021, **64**, 611–620.
- [9] Z. Gu, D. Bin, Y. Feng, K. Zhang, J. Wang, B. Yan, S. Li, Z. Xiong, C. Wang, Y. Shiraishi and Y. Du, *Appl. Surf. Sci.*, 2017, **411**, 379–385.
- [10] X. Yang, J. Xue and L. Feng, *Chem. Commun.*, 2019, **55**, 11247–11250.
- [11] S. Kang, G. Gao, X. Xie, T. Shibayama, Y. Lei, Y. Wang and L. Cai, *Mater. Res. Lett.*, 2016, **4**, 212–218.
- [12] J. Qiu, Y. Han, K. Zhang, Y. Deng, Y. Wu and L. Yan, *ACS Appl. Energy Mater.*, 2022, **5**, 4439–4447.
- [13] W. Tu, Y. Sun, D. Wu, H. Wang, H. Huang, M. Shao, Y. Liu and Z. Kang, *Mater. Chem. Phys.*, 2019, **225**, 64–71.
- [14] Z. Li, S. Xu, Y. Xie, Y. Wang and S. Lin, *Electrochim. Acta.*, 2018, **264**, 53–60.
- [15] Y. Chen, F. Niu, W. Sun, C. Liu, Y. Zhang, C. Xu, G. Ren, Z. Liu and X. Liu, *Chemistry Select.*, 2024, **9**, e202400519.
- [16] C. Luan, X. Zhang, C. Wang, M. Liao, W. Xu and B. Chen, *New J. Chem.*, 2023, **47**, 15711–15720.
- [17] S. Han, Y. Ma, Q. Yun, A. Wang, Q. Zhu, H. Zhang, C. He, J. Xia, X. Meng, L. Gao, W. Cao and Q. Lu, *Adv. Funct. Mater.*, 2022, **32**, 2208760.
- [18] J. Huang, Y. Liu, M. Xu, C. Wan, H. Liu, M. Li, Z. Huang, X. Duan, X. Pan and Y. Huang, *Nano*

Lett., 2019, 19, 5431–5436.

- [19] X. Wang, M. Xie, F. Lyu, Y. Yiu, Z. Wang, J. Chen, L. Chang, Y. Xia, Q. Zhong, M. Chu, H. Yang, T. Cheng, T. Sham and Q. Zhang, *Nano Lett.*, 2020, 20, 7751–7759.
- [20] Z. Chen, D. Rao, J. Zhang, Y. Liu, Y. Wang, C. Liu, W. Hu and Y. Deng, *ACS Appl. Energy Mater.*, 2019, 2(7), 4763–4773.
- [21] G. Liu, W. Zhou, Y. Ji, B. Chen, G. Fu, Q. Yun, S. Chen, Y. Lin, P. Yin, X. Cui, J. Liu, F. Meng, Q. Zhang, L. Song, L. Gu and H. Zhang, *J. Am. Chem. Soc.*, 2021, 143(29), 11262–11270.
- [22] F. Ma, R. Jin, K. Zhou, Y. Zhu, T. Huang, Q. Lu, L. Gai, L. Liu, R. Varma and K. Eid, *Chem. Eng. J.*, 2024, 492, 151988.
- [23] J. Zhang, M. Yuan, T. Zhao, W. Wang, H. Huang, K. Cui, Z. Liu, S. Li, Z. Li and G. Zhang, *J. Mater. Chem. A*, 2021, 9, 20676–2068.
- [24] X. Wang, Y. Liu, X. Ma, L. Chang, Q. Zhong, Q. Pan, Z. Wang, X. Yuan, M. Cao, F. Lyu, Y. Yang, J. Chen, T. Sham and Q. Zhang, *Nano Lett.*, 2023, 23, 685–693.
- [25] F. Zhao, J. Ye, Q. Yuan, X. Yang and Z. Zhou, *J. Mater. Chem. A*, 2020, 8, 11564–11572.